Thermodynamic properties in quantum dot nanocomposite for white light-emitted diodes

Phuc Dang Huu[1], Phan Xuan Le[2]
[1]Faculty of Fundamental Science, Industrial University of Ho Chi Minh City, Ho Chi Minh City, Vietnam
[2]Faculty of Mechanical-Electrical and Computer Engineering, School of Engineering and Technology, Van Lang University, Ho Chi Minh City, Vietnam

Article Info

Article history:

Received Oct 29, 2021
Revised May 11, 2022
Accepted Jun 19, 2022

Keywords:

Color homogeneity
Luminous flux
Monte Carlo theory
Quantum dot
WLEDs

ABSTRACT

For a colour conversion substance, we developed a new nanocomposite containing a CdSe/CdS/ZnS red-emitted quantum dot (QD), a green-emittedd Sr_2SiO_4:Eu phosphorus, and silicon resins. Regarding QD concentration and ingredients, the heat increase and optic features of the nanocomposite attributable to the QD inclusion were examined. According to the findings, a modest portion of QDs added to a photon converter at the emission wavelength of QD produced a considerable degree of heat. We used 0.2 wt% QDs over an InGaN blue-emitting light-emitted diodes (LED) chip to simulate a thermal increase in a nanocomposite. Consequently, we were able to produce a white-emitted LED module featuring a good 83.2 colour rendered index, an excellent 65.86 lm W-1 brightness, and a reasonable 94 °C thermal rise. The recently founded QD-phosphorus nanocomposite transformed white-emitted LED offers a lot of possibility of modern lighting.

Corresponding Author:

Phan Xuan Le
Faculty of Mechanical-Electrical and Computer Engineering, School of Engineering and Technology
Van Lang University
Ho Chi Minh City, Vietnam
Email: le.px@vlu.edu.vn

1. INTRODUCTION

Given their excellent efficacy, extended longevity, minimal energy consumption, rapid responsive rate, and dependability, white light-emitted diodes (WLEDs) have piqued attention for solid-state illuminating devices [1], [2]. WLEDs are by far the most viable replacement for traditional illumination supplies in various applications, namely conventional illumination, backlighting, indoor illumination, and branding [3]. Light-emitted diodes (LEDs) are used to produce white-emitting light in two ways. One option is to combine emissions from several colored lighting resources, including red, green, and blue emitting LED chips. The alternative option is to mix blue-emitted LED chips and a polymer matrix with $Y_3Al_5O_{12}:Ce^{3+}$ (YAG:Ce) phosphorus that emits yellow light. Owing to its great illuminating efficacy and intensity, basic construction, and reduced manufacturing expense in comparison with multi-chip WLEDs, phosphorus-converting WLEDs are mostly employed in commercial implementations [4]. Yet, the illumination generated by YAG:Ce-based WLEDs is cooler and more blue than that generated by incandescent lights, having a lower chromatic renderred indices (CRI) owing to the unavailability of green and red output elements, and the colour fidelity changes depending on the power supply [5]. To increase WLEDs' CRI, red-emitted phosphorus could be incorporated into the yellow-emitted one, though this is also troublesome in actual deployments [6], [7]. Semiconductor nanocrystals, commonly known as quantum dots (QDs), have sparked scientific and industry attention for a potential component in WLEDs colour conversion. Colloid

QDs have a variety of appealing features, comprising nanometer scale measurement, excellent photoluminescent (PL) quantum values, a broad absorbance spectra, a confined emitting region, reduced optical dispersion, and size-adjustable optic features [8]-[11]. Cd-based center, core-shell, and core-multicover QDs have been employed for WLED's colour rendition in earlier studies [8], [12]-[14]. Kozacki *et al.* [15] produced WLEDs lacking phosphors utilizing core–multicover QD elements. By combining red CdSe QDs with greenish-yellow-emitting $Sr_3SiO_5:Ce^{3+}$, Li^+ in LEDs, Han *et al.* [16] obtained good colour rendered performances. Employing yellow YAG:Ce phosphorus, red InP-based QDs, and green $Sr_{0.94}Al_2:Eu_{0.06}$ phosphorus, Kwon *et al.* [17] earned good CRI of WLED. Lecca *et al.* [18] and Elkarim *et al.* [19] created a WLED comprising green, red CdSe/ZnS core-cover QDs and an InGaN/GaN blue-emitted light.

The novel colour conversion substance, which is a blend of Sr_2SiO_4:Eu and CdSe/CdS/ZnS core-multicover red-emitted QD, has been tested in the article. Additionally, we initially detailed the QD nanocomposite's thermodynamic characteristics as a colour conversion element. We discovered that the QD concentration had a significant impact on both PL deterioration and thermal expansion of the nanocomposite. In addition, QDs function and impact over WLED gadgets of PL, correlation colour temperature (CCT), CRI, and illuminating efficacy were explored. Eventually, we showed great WLED featuring a 83.2 CRI, a 65.86 lm W^{-1} brightness, and a 94 °C circuit temperature.

2. RESEARCH METHOD

2.1. Compositions and their properties

QD solutions Co. (Korea) provided a 624 nm wavelength of red-emitting CdSe/CdS/ZnS core-multicover QDs, which were employed without adjustment. A Scinco SD-1000 UV-vis spectrophotometer was used to analyze UV-vis absorbance spectrum. A horiba fluorolog spectrometer was used to measure PL spectrum at ambient temperature namely 50, 100, and 150 °C with a xenon projector as resource of excitation; the examination was completed after an one-hour heat treatments and ambient quenching [20]. At 300 kV, an FEI Tecnai G^2F30 S-Twin gadget was used to acquire transmitted electron microscope (TEM) pictures. To fabricate the specimens, QDs were distributed in toluene and placed on 300-mesh perforation carbon panels. The green Sr_2SiO_4:Eu phosphorus's PL spectrum featuring a peak 519 nm excitation were calculated. Trikaiser provided InGaN-based blue-emitted LED chips (NLX-5 blue power die, λ_{max} value = 455 nm, non-epoxy shaping packages). Dow corning supplied the double-element heat-curable silicon resins (OE-6630 A and B).

2.2. Mixing QD-phosphorus in polymer and the implementation on LEDs

To eliminate unwanted imperfections, we combined the silicon epoxy components A and B in a 1:4 volume ratio and deposited the solution in a pressure heater for half an hour at 1 bar. Next, 0.03 g (10 wt%) of phosphorus and 0.000 6 g (0.2 wt%) of QD in toluene solvent were blended in 0.3 g of silicon epoxy and also set in a pressure tube to discard the toluene and bubbling. Then the solution was withdrawn, compound sheets were made, and PL emitted from the core-multicover QD nanocomposite and from the phosphorus were monitored prior and post-treating. The QD-phosphorus-silicon combination was deposited over blue-emitted LED chips and heat-treated around 150°C in an hour to make the QD-phosphorus-converted WLEDs. WLEDs optic properties, including electroluminescence (EL), luminescent efficacy, chroma temperature, and the Commission Internationale de l'Eclairage (CIE) chromatic coordinates, were assessed employing a Photoresearch PR650 Spectrascan sensor at ambient temperature and functioning current flow ranging from 40 to 400 mA. At ambient temperature, CRI properties were calculated utilizing a Labsphere SLMS LED 1060 instrument. With a forward-looking infrared radiometer (FLIR) A320 infrared recording device, the heat dispersion throughout the WLED chips were continually monitored.

3. RESULTS AND DISCUSSION

3.1. QD's optic properties, phosphorus and QD-phosphorus-resin composite

Identifying an adequate host polymeric matrix which is able to sustain the original PL intensity is the primary objective in the synthesis of QD-based materials for illumination converting purposes. The availability of the silicon resin synthesized had no significant effect over the PL intensity or QDs spectroscopic peak. The lower absorption generated from back-scatter process in the host matrix is probably the reason of a moderate reduction in the PL intensity of QDs in resinous combinations (not illustrated in this). The red-band PL emitted spectrum steadily rose with the QD content, and the ratio of the PL region of phosphorus and that of QDs climbed from 1:0.10 to 1:0.21 and to 1:0.28. The proportion of PL intensity amplification because of QD inclusion, on the other hand, reduced. That is likely to probable since the addition of excessive QDs disrupted the QDs distribution inside the viscous host matrices, resulting in a decline or suppression of the photoluminescence. The proportions of phosphorus PL region and QDs altered following the curing procedure are 1:0.09, 1:0.18, and 1:0.23, equivalent to QD concentrations of 0.2, 0.6, and 1.0 wt%, accordingly. In comparison to the uncured form, the red-band PL region was decreased by 7.0%, 14.2%, and 20.7%. This reduction in the red-emitted zone PL region is probably owing to strong curing permanently damaging certain QDs. In comparison to the uncured example, the red-colored output associated to the core-multicover QDs changed into a greater wavelength (for example from 624 to 627 nm).

3.2. LED, thermal impacts of QD, and nanocomposite

When the QD solution temperature grew, the remedy's PL intensity fell. The PL spectroscopic maxima also responded to heat in a reverse manner. Once the QD solution was agitated, the PL region moved nearer the red band thereafter restored upon cooling down [21], [22]. At 150 ºC, the persistent shift in PL intensity owing to high-heat treatment was found to be around 8.4%, which was similar to the PL emitted spectrum of phosphorus composites and core-multicover QDs following the procedure curing. As a result, high-heat conditions should be prevented when using QDs. Similarly, the excessive heat would have negative consequences on both the silicon resins and the phosphorus.

We removed the polymer component in shape of a cup to place the chromatic conversion substance on a LED module to check the thermal increase of the nanocomposite owing to the inclusion of QD and/or phosphorus in silicon resins. The translucent sliding glass was mounted to the bottom-less plastic container, and the resins either with or without QD and/or phosphorus was placed. The UV optic link was placed and secured underneath the slide at a 50 mm length, making direct thermal conversion from the UV supply towards the nanocomposite impossible. We show a diagram of illumination conversion and thermal dissipation channels. As UV radiation is shown on a restricted nanostructure, some of it passes across the resin or either is converted towards a different wavelength via the QD, while the remainder is dissipated owing to the back and sides scattering caused by reflection, dispersion, and diffraction, among other things. During the illuminated conversion and transmission, heat is produced simultaneously [23]. We discovered that the temperature generated by QDs was substantially greater compared to that produced by the resins and phosphorous. We also examined the UV resource's thermometer and the glass substrate to investigate the ecological impact. After 5 minutes, the resin's thermal increase was around 55 °C, lower than the UV resource's one (85 °C).

Numerous mixes containing a luminous substance, including QD and phosphorus, had substantially greater temperatures than the resins alone. Across all combination circumstances, a QD-only implanted nanostructure culminated in the largest thermal gain. In the secondary photon discharge off the QDs, the obtained photon energy of the QD is dissipated into heat due to electron-photon scatter. Although the mass ratio of QDs in the resin was significantly smaller compared to that of phosphorus, QDs generated significantly more heat compared to phosphorus. The thermal gain of the nanostructure was smaller than those of QDs alone, but greater than those of phosphors itself once both the QDs and phosphors were blended in the resins substrate. It indicates that if absorbed illumination is transformed by the phosphorus and QD, the temperature generated by the QDs' illumination transmission contributes more to the resins.

Figure 1 shows the reversal shift in the concentrations of green-emitted QD and yellow-emitted $YAG:Ce^{3+}$ phosphors. This adjustment has several interpretations: first, it maintains average CCTs, secondly, it impacts two-layered phosphorus WLEDs scatter and absorbance. Such, in turn, has an impact on WLEDs chromatic quality and illuminating flux efficacy. WLEDs chromatic quality is therefore determined by the QD concentration chosen. As 2% in the QD concentration rises to 20% wt, that of $YAG:Ce^{3+}$ decreased to maintain the median CCTs. This is also true for WLEDs having colour temperatures ranging between 5600 and 8500 K.

Figure 2 depicts the influence of the green-emitted QD phosphorous concentration on WLEDs transmission spectra. It is feasible to decide based upon the manufacturer's specifications. WLEDs that demand good colour fidelity can diminish illuminating flux by a minuscule portion. As shown in Figure 2, white-emitted light is the spectral area's composition. The spectrum in the five following values are 5600, 6600, 7000, 7700, and 8500 K, accordingly. Clearly, the amplitude pattern increases with QD concentration in two sections of the optical spectral range: 420-480 nm and 500-640 nm. The rise in the discharged illuminating flux may be seen in the two-band emitting spectra. Furthermore, blue-light diffraction within WLEDs is enhanced, implying that diffraction throughout the phosphorus layer and WLEDs is improved as well, favoring chromatic homogeneity. If QD is used, this is a significant outcome. The colour consistency of the extreme heat remote phosphorus configuration, is challenging to manage. This analysis revealed that QD, at both high and low color temperatures (8500 and 5600 K), can improve WLEDs chromatic fidelity.

The efficacy of the diffracted illuminating flux of this double-layer remote phosphorus layer was thus demonstrated in the article. The findings in Figure 3 illustrate that if 2% wt. of QD concentration is adjusted to 20% wt, the illuminating flux emission increases dramatically. Throughout three median CCTs, the colour variation was massively diminished as QD phosphorus concentration, as shown in Figure 4. This can be explained by the red-emitted phosphorus layer's absorbance. Once the blue emission from the LED chip is absorbed by the QD phosphorus, it is converted into green. The yellow-emitted light is absorbed by the QD ions in complement to the LED chip blue-emitted light. The blue-emitted illumination absorbance from LED's chip, though, is stronger than these two absorptions due to the substance's absorbance qualities. As a result of the introduction of QD, the green-emitted light percentage in WLEDs increases, improving the chromatic homogeneity indicator. Chromatic uniformity is among the most important factors across current WLED lighting criteria. The better the chromatic uniformity rating, the more expensive WLED white-emitted light is. Yet, the efficient price of QD is a plus. QD could therefore be employed in a variety of applications.

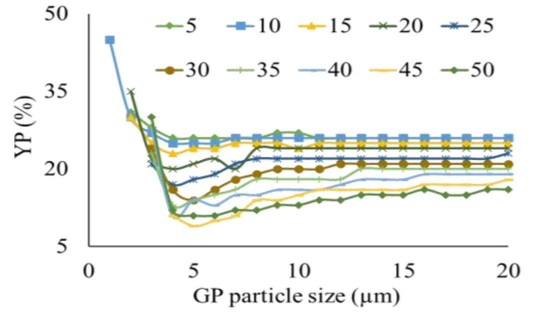

Figure 1. Maintaing the median CCT by modifying the phosphorus concentration

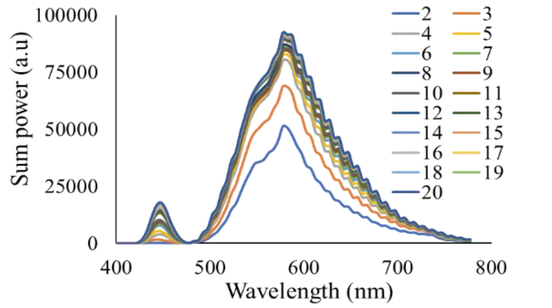

Figure 2. QD concentration functions as WLEDs 3000 emitting spectrum

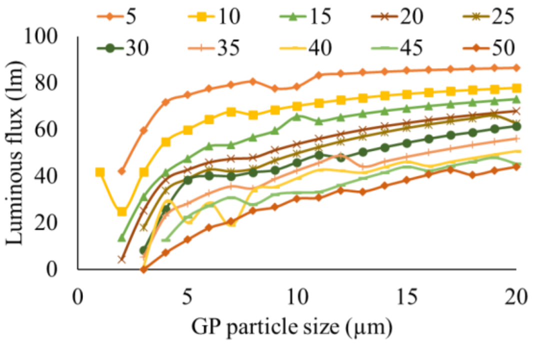

Figure 3. QD concentration functions as WLEDs luminous flux

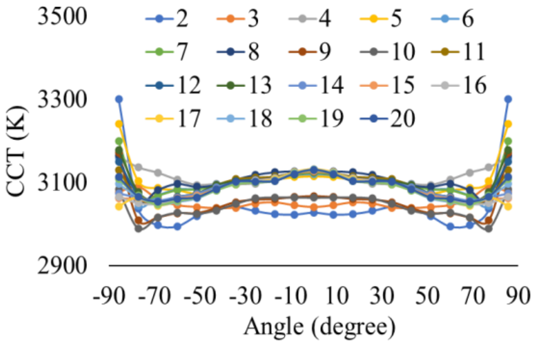

Figure 4. QD concentration functions as WLEDs CCT

Chromatic uniformity is merely a single criterion to consider when assessing WLED colour fidelity. Colour fidelity is not excellent as color uniformity rate is high. As a result, subsequent investigations have developed a colour rendered index and a chromatic fidelity score. If light is shining on the colour rendered index, it determines the genuine chromaticity. The overwhelming abundance of green-emitted light among the principal shades: blue, yellow, and green, causing the colour imbalance. This, too, has an effect on WLEDs colour fidelity, resulting in a decrease. The data in Figure 5 show a small decline in CRI with addition of the distant phosphorus QD layer. Color quality score/scale (CQS) is more significant and more difficult to attain in comparison with CRI. CQS is a three-factor indicator, including the colour rendered index, the user's preferred choice, and the color coordinates. For such important indicators, CQS is basically a genuine overall assessment of colour fidelity [24], [25]. Figure 6 shows CQS's improvement with the addition of the remote QD phosphorus layer. Furthermore, CQS does not vary substantially if QD concentration is raised to under 10% wt. CRI and CQS are greatly diminished as QD concentrations are over 10% wt. suffering from severe coloration reduction if green content is dominating. As a result, while using green-emitted QD phosphorus, proper concentration preference is critical.

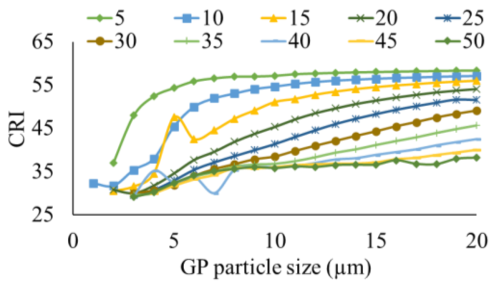

Figure 5. QD concentration functions as WLEDs chromatic rendered index

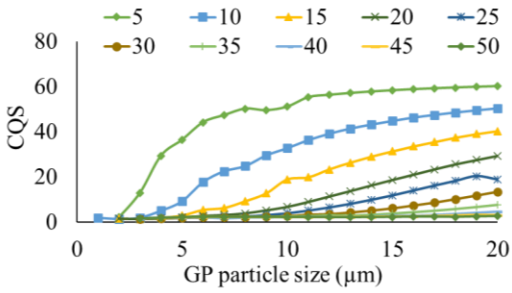

Figure 6. QD concentration functions as WLEDs chromatic quality scale

4. CONCLUSION

The effect of the green-emitted QD phosphor on the optic properties of a double-layer phosphorous arrangement is discussed in this work. The analysis revealed that QD is a great option to optimize chromatic homogeneity relying on Monte Carlo computational simulations. This is applicable for WLEDs featuring a low 5600 K colour temperature as well as those of exceeds 8500 K. The outcomes of this study have so achieved the goal of improving chromativ fidelity and illuminating flux, which is difficult to do due to the remote arrangement of phosphor. Nonetheless, CRI and CQS have a slight drawback. The CRI and CQS fall dramatically as QD concentration is elevated substantially. As a result, the right concentration must be chosen on the basis of manufacturer's aims. The research has a tremendous amount of useful data for generating better WLEDs colour homogeneity and illuminating flux. To summarize, we created a unique nanoparticle for a colour conversion substance by integrating red-emitted QD and green-emitted phosphorus in a silicon epoxy. The optic properties of QD and phosphorus were investigated in terms of absorbance and PL. We discovered that increasing the amount of QD in the phosphorus-resin combination improved the luminous region of PL across the QD spectrum wavelength. As we irradiated the nanostructure with Ultraviolet rays, the QD and phosphorus within the resin produced a lot of heat. Despite the fact that QDs had a lower concentration than phosphorus, the temperature increase caused by QDs was substantially greater. Similarly, as we used this nanostructure to create white emission in an LED gadget, the equivalent thing happened in terms of heat properties. When 1, 0.6, and 0.2 wt% QD are added to the LED circuit, the temperatures goes to 94, 109, and 131 °C, accordingly. The optic efficiency of WLEDs was determined using the QDs concentration. WLED featuring 0.2 wt% QDs generated illumination having 0.2988, 0.3283 in CIE coordinates, a 94 °C gadget temperature, a 6672 K CCT, a 65.86 lm W^{-1} illuminating efficacy, and a 83.2 CRI. It is likely to be employed as a general lighting resource and can handle extreme-power uses.

ACKNOWLEDGEMENTS

This study was financially supported by Van Lang University, Vietnam.

REFERENCES

[1] X. Leng *et al.*, "Feasibility of co-registered ultrasound and acoustic-resolution photoacoustic imaging of human colorectal cancer," *Biomed. Opt. Express*, vol. 9, no. 11, pp. 5159-5172, Oct. 2018, doi: 10.1364/BOE.9.005159.

[2] Y. Tang, Z. Li, G. Liang, Z. Li, J. Li, and B. Yu, "Enhancement of luminous efficacy for LED lamps by introducing polyacrylonitrile electrospinning nanofiber film," *Opt. Express*, vol. 26, no. 21, pp. 27716-27725, Oct. 2018, doi: 10.1364/OE.26.027716.

[3] X. Bao, X. Gu, and W. Zhang, "User-centric quality of experience optimized resource allocation algorithm in VLC network with multi-color LED," *Opt. Express*, vol. 26, no. 21, pp. 27826-27841, Oct. 2018, doi: 10.1364/OE.26.027826.

[4] B. Li *et al.*, "High-efficiency cubic-phased blue-emitting Ba3Lu2B6O15:Ce3+ phosphors for ultraviolet-excited white-light-emitting diodes," *Opt. Lett*, vol. 43, no. 20, pp. 5138-5141, Oct. 2018, doi: 10.1364/OL.43.005138.

[5] V. B. Yekta and T. Tiedje, "Limiting efficiency of indoor silicon photovoltaic devices," *Opt. Express*, vol. 26, no. 22, pp. 28238-28248, Oct. 2018, doi: 10.1364/OE.26.028238.

[6] W. J. Kim, T. K. Kim, S. H. Kim, S. B. Yoon, H. H. Jeong, J. O. Song, and T. Y. Seong, "Improved angular color uniformity and hydrothermal reliability of phosphor-converted white light-emitting diodes by using phosphor sedimentation," *Opt. Express*, vol. 26, no. 22, pp. 28634-28640, Oct 2018, doi: 10.1364/OE.26.028634.

[7] Y. Xie *et al.*, "Encapsulated room-temperature synthesized CsPbX3 perovskite quantum dots with high stability and wide color gamut for display," *Opt. Mater. Express*, vol. 8, no. 11, pp. 3494-3505, Nov. 2018, doi: 10.1364/OME.8.003494.

[8] M. A. Juratli *et al.*, "Noninvasive label-free detection of circulating white and red blood clots in deep vessels with a focused photoacoustic probe," *Biomed. Opt. Express*, vol. 9, no. 11, pp. 5667-5677, Nov. 2018, doi 10.1364/BOE.9.005667.

[9] D. Molter, M. Kolano, and G. V. Freymann, "Terahertz cross-correlation spectroscopy driven by incoherent light from a superluminescent diode," *Opt. Express*, vol. 27, no. 9, pp. 12659-12665, Apr. 2019, doi: 10.1364/OE.27.012659.
[10] A. Ali *et al.*, "Blue-laser-diode–based high CRI lighting and high-speed visible light communication using narrowband green-/red-emitting composite phosphor film," *Appl. Opt,* vol. 59, no. 17, pp. 5197-5204, Jun. 2020, doi: 10.1364/AO.392340.
[11] S. Beldi *et al.*, "High Q-factor near infrared and visible Al_2O_3-based parallel-plate capacitor kinetic inductance detectors," *Opt. Express*, vol. 27, no. 9, pp. 13319-13328, Apr. 2019, doi: 10.1364/OE.27.013319.
[12] C. H. Lin, A. Verma, C. Y. Kang, and Y. Pai, "Hybrid-type white LEDs based on inorganic halide perovskite QDs: candidates for wide color gamut display backlights," *Photon. Res,* vol. 7, no. 5, pp. 579-585, May. 2019, doi: 10.1364/PRJ.7.000579.
[13] S. R. Chung, C. Siao, and K. W. Wang, "Full color display fabricated by CdSe bi-color quantum dots-based white light-emitting diodes," *Opt. Mater. Express*, vol. 8, no. 9, pp. 2677-2686, Aug. 2018, doi: 10.1364/OME.8.002677.
[14] J. Zhang, L. Zhao, X. Bian, and G. Chen, "Ce3+/Mn2+-activated Ca7(PO4)2(SiO4)2: efficient luminescent materials for multifunctional applications," *Opt. Express,* vol. 26, no. 18, pp. A904-A914, Sep. 2018, doi: 10.1364/OE.26.00A904.
[15] T. Kozacki, M. Chlipala, and H. G. Choo, "Fourier rainbow holography," *Opt. Express*, vol. 26, no. 19, pp. 25086-25097, Sep. 2018, doi: 10.1364/OE.26.025086.
[16] C. Han *et al.*, "Effect of surface recombination in high performance white-light CH3NH3PbI3 single crystal photodetectors," *Opt. Express*, vol. 26, no. 20, pp. 26307-26316, Oct. 2018, doi: 10.1364/OE.26.026307.
[17] O. H. Kwon, J. S. Kim, J. Jang, and Y. Cho, "Simple prismatic patterning approach for nearly room-temperature processed planar remote phosphor layers for enhanced white luminescence efficiency," *Opt. Mater. Express,* vol. 8, no. 10, pp. 3230-3237, Oct. 2018, doi: 10.1364/OME.8.003230.
[18] M. Lecca, "Generalized equation for real-world image enhancement by Milano Retinex family," *J. Opt. Soc. Am. A,* vol. 37, no. 5, pp. 849-858, May. 2020, doi: 10.1364/JOSAA.384197.
[19] M. A. Elkarim, M. M. Elsherbini, H. M. AbdelKader, and M. H. Aly, "Exploring the effect of LED nonlinearity on the performance of layered ACO-OFDM," *Appl. Opt,* vol. 59, no. 24, pp. 7343-7351, Aug. 2020, doi: 10.1364/AO.397559.
[20] F. Brusola, I. Tortajada, I. Lengua, B. Jordá, and G. P. Fajarnés, "Parametric effects by using the strip-pair comparison method around red CIE color center," *Opt. Express,* vol. 28, no. 14, pp. 19966-19977, Jul. 2020, doi: 10.1364/OE.395291.
[21] B. H. Q. Thang *et al.*, "High-performance nanowire ultraviolet light-emitting diodes with potassium hydroxide and ammonium sulfide surface passivation," *Appl. Opt*, vol. 59, no. 24, pp. 7352-7356, Aug. 2020, doi: 10.1364/AO.400877.
[22] Z. Zhang, and W. Yang, "Tunable photoluminescence in $Ba_{1-x}SrxSi_3O_4N_2$: Eu^{2+}/ Ce^{3+}, Li^+ solid solution phosphors induced by linear structural evolution," *Opt. Mater. Express,* vol. 9, no. 4, pp. 1922-1932, Apr. 2019, doi: 10.1364/OME.9.001922.
[23] T. W. Kang *et al.*, "Enhancement of the optical properties of $CsPbBr_3$ perovskite nanocrystals using three different solvents," *Opt. Lett,* vol. 45, no. 18, pp. 4972-4975, Sep. 2020, doi: 10.1364/OL.401058.
[24] G. Prabhakar, P. Gregg, L. Rishoj, P. Kristensen, and S. Ramachandran, "Octave-wide supercontinuum generation of light-carrying orbital angular momentum," *Opt. Express,* vol. 27, no. 8, pp. 11547-11556, Apr. 2019, doi: 10.1364/OE.27.011547.
[25] R. Dang, H. Tan, N. Wang, G. Liu, F. Zhang, and X. Song, "Raman spectroscopy-based method for evaluating LED illumination-induced damage to pigments in high-light-sensitivity art," *Appl. Opt,* vol. 59, no. 15, pp. 4599-4605, May. 2020, doi: 10.1364/AO.379398.

BIOGRAPHIES OF AUTHORS

Phuc Dang Huu received a Physics Ph.D degree from the University of Science, Ho Chi Minh City, in 2018. Currently, he is a lecturer at the Faculty of Fundamental Science, Industrial University of Ho Chi Minh City, Ho Chi Minh City, Vietnam. His research interests include simulation LEDs material, renewable energy. He can be contacted at email: danghuuphuc@iuh.edu.vn.

Phan Xuan Le received a Ph.D. in Mechanical and Electrical Engineering from Kunming University of Science and Technology, Kunming city, Yunnan province, China. Currently, He is a lecturer at the Faculty of Engineering, Van Lang University, Ho Chi Minh City, Viet Nam. His research interests are Optoelectronics (LED), Power transmission and Automation equipment. He can be contacted at email: le.px@vlu.edu.vn.